Journal of Membrane Science 652 (2022) 120492

Contents lists available at ScienceDirect

Journal of Membrane Science

journal homepage: www.elsevier.com/locate/memsci

B-oriented MFI zeolite membranes for xylene isomer separation - Effect of xylene activity on separation performance

Fateme Banihashemi, Jerry Y.S. Lin *

School of Engineering for Matter, Transport and Energy, Arizona State Universtiy, Tempe, AZ, 85287, United States

ARTICLE INFO

Keywords:
Zeolite membranes
B-orientation
Xylene separation
Vapor permeation
Pervaporation

ABSTRACT

MFI zeolite membranes, especially b-oriented ones, show superb vapor permeation/separation performance for xylene isomer separation at low vapor pressures. In industrial applications these membranes should be operated at high xylene vapor pressures in the vapor separation mode or with liquid feed in the pervaporation mode. This paper reports the influence of xylene activity on xylene vapor and liquid permeation/separation performance of b-oriented MFI zeolite membranes. High quality b-oriented MFI zeolite membranes were synthesized with an organic template on modified silica substrates. For vapor permeation with binary p/o-xylene feed, both permeance (for p-xylene and o-xylene) and p-/o-xylene separation factor increase, with separation factor reaching maximum of 515 at 150°C, then decreases with increasing temperature due to combined effects of temperature dependence of diffusivity and adsorption. The vapor permeance for both xylenes and separation factor decrease monotonically with increasing xylene activity (or vapor pressure). Lowest separation factor is observed when operated in the pervaporation mode giving p-/o-xylene separation factor of about 2. Compared to randomly oriented MFI zeolite membranes synthesized with an organic template, the b-oriented MFI zeolite membranes show better vapor permeation/separation performance and less negative effect of xylene activity on separation factor. However, both b- and randomly oriented MFI zeolite membranes exhibit a similarly poor separation factor when operated in the pervaporation mode.

1. Introduction

Separation of xylene isomers is one of most energy intensive processes in the petrochemical industry [1,2]. Membrane separation is an attractive alternative to the current energy-intensive traditional separation processes such as distillation, crystallization or adsorption, for xylene separation [3]. MFI type zeolite membranes offer great potential in separation of xylene isomers by a membrane process [4]. Recently, b-oriented zeolite membranes have offered attractive separation performance for separating p-xylene over xylene isomer mixture at the low xylene partial pressures [5]. The experimental and simulation data [6,7] show that b-oriented MFI zeolite membranes have higher p-xylene separation factor than randomly oriented ones at low xylene vapor pressure because of the fact that the straight channels along the b-axis could be the quickest diffusion pathway in MFI zeolite crystals for p-xylene [8,9].

Yoon and co-workers [10,11] synthesized good quality b-oriented MFI zeolite membranes for xylene isomers separation on porous silica substrates respectively by the secondary growth gel and gel-free methods. They reported high separation factor for vapor permeation separation of p-xylene/o-xylene by such b-oriented MFI zeolite membranes at various temperature ranges (480 at 200 °C [12], 1100 at 150 °C [10,11], and 2500 at 120 °C [13]). Tsapatsis and co-workers [14] reported vapor permeation p-xylene/o-xylene separation factor up to 8000 and maximum p-xylene permeance of 2.9×10^{-7} mol m^{-2} $s^{-1}Pa^{-1}$ in 100–175 °C for a b-oriented MFI membrane synthesized by floating coating of MFI-zeolite nanosheets followed by gel-free secondary growth. All the above xylene separation results on b-oriented MFI membranes were attained by vapor permeation method at very low xylene partial pressures (<1 kPa). However, the effect of xylene vapor pressure (or xylene activity defined as the ratio of the actual partial pressure to the saturated vapor pressure) on xylene vapor permeation/separation performance of b-oriented MFI zeolite membrane is not clear. To date, no pervaporation xylene separation data have been reported for b-oriented MFI zeolite membranes. The pervaporation experiments can be considered as vapor permeation at the saturated vapor pressure, or at the unity activity.

The xylene activity has a strong effect on xylene separation

---

* Corresponding author.
E-mail address: Jerry.Lin@asu.edu (J.Y.S. Lin).

https://doi.org/10.1016/j.memsci.2022.120492
Received 11 February 2022; Received in revised form 19 March 2022; Accepted 22 March 2022

performance on randomly oriented MFI zeolite membranes [15–17]. Lin and his co-workers [15] studied the effects of xylene activity and membrane microstructure on separation performance in xylene vapor permeation and pervaporation modes. Their results showed both p-xylene and o-xylene permeances decrease with increasing xylene activity from 0.008 to 0.033, but the decrease is more pronounced for p-xylene resulting in a reduction in p-xylene/o-xylene selectivity. Additionally, they documented minimization of intercrystalline gaps not only improves the p-xylene/o-xylene selectivity but also weakens the unfavourable activity dependence of xylene permeance and selectivity for the randomly oriented MFI zeolite membranes. Falconer and co-workers [16] reported a decrease of p-xylene/o-xylene separation factor by 70% with feed partial pressure of xylene increasing from 0.4 to 2.5 kPa (activity increasing from 0.00296 to 0.018). Dong and co-workers [17] observed 50% decrement in p-xylene/o-xylene separation factor and 20% increment in p-xylene flux with an increase in xylene partial pressure from 0.91 to 87.2 kPa (increase in activity from 0.0009 to 0.087).

Increasing xylene activity means increasing loading of xylene in the zeolite crystal framework of the zeolite membrane. At low feed xylene pressure, the o-xylene flux with binary p-xylene/o-xylene feed is very close to the single component value [9,17]. At higher feed pressure p-xylene sorption induces local distortions in the microstructure of MFI zeolite membrane, increasing the permeability for o-xylene through the zeolite pores. This results in a decrease in the p-xylene/o-xylene separation factor for the randomly oriented MFI zeolite membranes [9,17,18]. For the b-oriented MFI zeolite membranes, Tsapatsis and co-workers [5] also reported a 40% decrease in p-xylene/o-xylene separation factor from 1989 to 1167 with an increase in p-xylene partial pressure from 0.37 to 0.42 kPa (activity increasing from 0.0027 to 0.0031) at 150 °C.

In industrial process separation of xylene mixture by membranes will be conducted either by vapor permeation at high vapor pressure (or activity), or preferably, by pervaporation with liquid feed (activity equal to unity). However, for highly selective b-oriented MFI zeolite membranes the details of such effects of xylene activity on membrane performance are not known and no xylene pervaporation separation data is available. Herein we report an experimental study on xylene separation properties of the b-oriented MFI zeolite membranes operated in both pervaporation and vapor permeation modes to understand the effects of xylene activity on separation performance of b-oriented MFI zeolite membranes. The results are compared with separation properties of randomly oriented MFI zeolite membranes prepared with an organic template.

2. Experimental

Homemade macroporous silica fiber disk substrates of about 20 mm in diameter and 2–3 mm in thickness were prepared by the press and sintering method reported by Yoon and his coworkers [11] with minor modification, from quartz fibers (Technical Glass Products, coarse, 9 μm wool). To modify the silica fiber substrates, silica powders of three different sizes (1000, 350, and 50 nm) were synthesized in our lab according to the Stöber procedure [19] using two solutions with the compositions given in literature [20]. Tetraethyl orthosilicate (TEOS, 98%, Sigma Aldrich) and 200 proof ethanol were mixed separately in room temperature. This solution was added into the solution of ammonium hydroxide (NH_4OH, 28.0-30.0% NH3 basis, Sigma Aldrich), ethanol and distilled water. The resultant solution was stirred for 2h at room temperature. White colloidal particles formed in the solution were collected by centrifugation (10,000 rpm) and washed 3 times in ethanol. Particles were dried at 50 °C over night and were calcined in the furnace. To synthesize 1 μm silica particle, syringe pump was used for adding first solution to the second one under nitrogen atmosphear. The surface modification of the silica fiber substrates was performed by rubbing with the silica powders sequentially of decreasing particle sizes (1000, 350, and 50 nm).

A suitable polymeric intermediate layer was necessary to avoid seed slip on the modified silica fiber substrates after rubbing. The polymer solution was made by mixing a mixture of 50 wt % solution of polyacrylic acid (Sigma-Aldrich, Mw 1800) in water and 0.2 mL ethylene glycol (99.8%, Sigma-Aldrich) followed by sonication for 1h [20]. The obtained solution was spin-coated at 4,000 rpm for 15s on the modified silica substrates twice. Pure silica MFI zeolite (silicalite) solution was prepared by introducing tetraethyl orthosilicate (TEOS, 98%, Sigma Aldrich) into the solution containing tetra propylammonium hydroxide (TPAOH, 1 M, Sigma Aldrich) and H_2O with stirring for 24 h at room temperature, and then treated hydrothermally as explained in our previous publication [21]. The obtained silicalite crystals after washing and drying were then coated on the polymer coated silica substrate by the rubbing method. Silica fiber seeded substrates were calcined at 550 °C for 6 h with a heating and cooling rate of 0.5 °C/min.

MFI Zeolite seeded modified silica fiber substrates were dip-coated in an equimolar solution of tetra propyl ammonium bromide (TPABr, 98%, Sigma-Aldrich) and potassium hydroxide (KOH, 85%, Sigma-Aldrich) for 30s and then transferred to a Teflon-lined stainless-steel autoclave for hydrothermal treatment. After synthesis, the membranes were washed with de-ionized water and dried at room temperature for one day. B-oriented membranes were calcined at 400 °C for 12h for organic template removal. Table 1 summarize synthesis conditions for MFI zeolite seed crystals and B-oriented membranes prepared in this work.

The crystallinity and phase structure of the MFI zeolite membranes were characterized using X-ray diffraction (XRD, Bruker AXS-D8) with the scan step of 0.015°. Amray 1910 scanning electron microscope (SEM) was used to image membrane surface morphology and measure membrane thickness. Pervaporation experiments of xylene isomers were performed at room temperature using the setup depicted in Fig. 1. The liquid feed was maintained at atmospheric pressure and contained in the steel feed tank, but the permeation side was kept under vacuum. The permeate was continuously collected for 1h in a cold trap inserted in a liquid nitrogen jar.

Vapor permeation experiments were conducted in a Wicke-Kallenbach separation set-up illustrated schematically in Fig. 2. The feed and permeate sides were kept at atmospheric pressure and helium was used as the sweep gas. The temperature of the module was controlled between 298 and 498 K. Mass flow controllers were used to control He flow rate in each line. He as carrier gas was saturated with binary xylene vapor by bubbling it through xylene mixture in a saturator before being directed to the membrane module. The membrane module and the pipeline to the gas chromatograph (GC) were heated above the xylene boiling point temperature by the oven and heating tapes to prevent condensation of xylenes. The compositions of the feed and permeate streams in both pervaporation and vapor permeation experiments were analyzed using a GC [Agilent Technologies GC-6890 N with a flame ionization detector (FID) and an HP-5 capillary column]. The accuracy of pervaporation and vapor permeation results was ±3.0% for the permeation of pure components and ±5.0% for binary mixture separation data.

3. Results and discussion

The original silica fiber substrates prepared by the pressing and

Table 1
Synthesis conditions of MFI zeolite seeds and b-oriented membranes.

Sample	Solution composition	Temperature (°C)	Synthesis time (h)
Coffin shaped seeds	$6TEOS:1.28TPAOH:620H_2O$	150	2
B-oriented Membrane	0.075 M TPABr + 0.075 M KOH	185	48

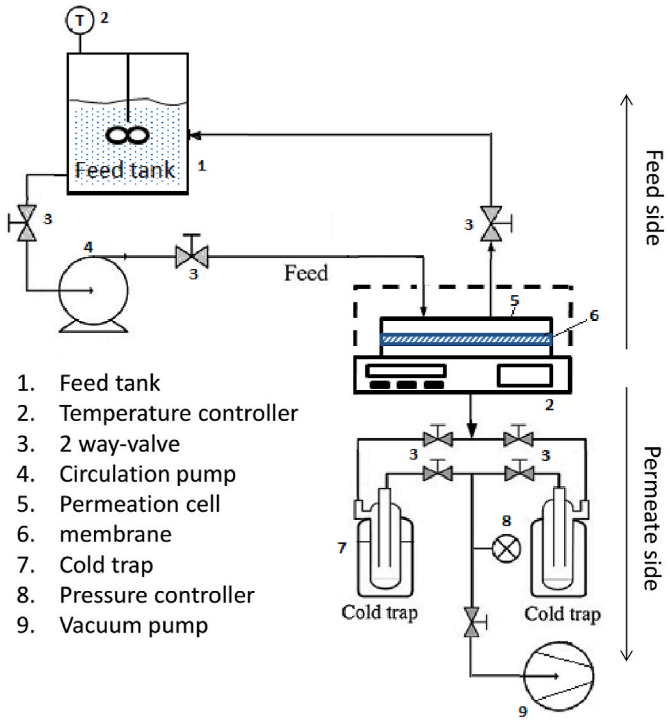

Fig. 1. Schematic diagram of xylene permeation/separation set-up for pervaporation experiments.

sintering process have a quite rough surface (Fig. 3A). The substrates have porosity, average pore diameter and tortuosity respectively of 40%, 840 nm and 2. A smooth and uniform surface of substrate was achieved after modification sequentially with 1 μm (Fig. 3B) 350 nm (Figs. 3C) and 50 nm silica powders (Fig. 3D) synthesized in this work. The modified silica supports have He permeance of 2.4 × 10^{-5} mol· Pa^{-1}·m^{-2}·s^{-1}, which is about two orders of magnitude higher than the helium permeance after formation of zeolite membrane layer. Thus, the support has negligible resistance in the final MFI zeolite membranes.

MFI zeolite crystals hydrothermally synthesized in this work are of coffin shape with average size of 1.5 × 0.6 × 1.9 μm^3 as shown in Fig. 4A. The MFI zeolite seed layer was coated by manually rubbing the coffin-shaped zeolite crystal powder on the modified silica fiber substrates. The surface micrograph (Fig. 4B) shows that the MFI zeolite crystals lay down flat and well aligned, similar to what was reported by Yoon, Tsapatsis and their co-workers [13]. XRD analysis of seeded substrate given in Fig. 5 show dominant peaks at two-theta of 8.92°, 17.82°, 26.87°, 36.09°, and 45.53° attributed to (0 2 0), (0 4 0), (0 6 0), (0 8 0) and (0 1 0 0) reflections of MFI zeolite crystals. The XRD data confirm that the MFI zeolite crystal seeds coated on the modified silica substrate are b-oriented with b-channel running normal to the support surface as reported by Tsapatsis and co-workers [5].

The surface and cross-sectional micrographs of MFI zeolite membrane after secondary growth (Fig.4C and D) show a well-intergrown MFI zeolite layer on top of the surface of the modified silica fiber substrate. The zeolite crystals have essentially same orientation and shape as the seed crystals but are larger in size (about 6–8 μm in length). From the side view SEM image showing a uniform zeolite membrane layer the thickness is estimated at about 1.2 μm. Comparing the XRD data of the MFI zeolite membrane after secondary growth with that of the seeded MFI zeolite layer (Fig. 5) shows appearance and intensification of the (0h0) diffraction peaks of the membrane after the secondary growth step. All these data show that the secondary growth step leads to monolayer, highly b-oriented and well-intergrown MFI zeolite membranes on the silica supports.

Fig. 6A shows binary-component permeation/separation data for the b-oriented MFI zeolite membrane in the temperature range of 125–200 °C. Similar results for the templated random membrane [15] are also given for comparison (Fig. 6B). The permeance for both p-xylene and o-xylene increases first and then decreases with increasing temperature, with a maximum at 150 °C. The temperature dependence of p-xylene permeance and p-/o-xylene separation factor of synthesized b-oriented membrane is similar to the results reported by Tsapatsis and co-workers [14] for their b-oriented MFI zeolite membrane and the high quality randomly oriented MFI zeolite membrane synthesized by the template-free method reported by our group [15].

The permeation of xylene isomers in MFI zeolite layer is controlled by an adsorption-diffusion mechanism in which adsorption equilibrium constant decreases while diffusivity increases with increasing temperature [15]. Consequently, there is a maximum in p-xylene/o-xylene permeance and selectivity at a given temperature for high quality MFI zeolite membranes. For MFI zeolite membranes with more

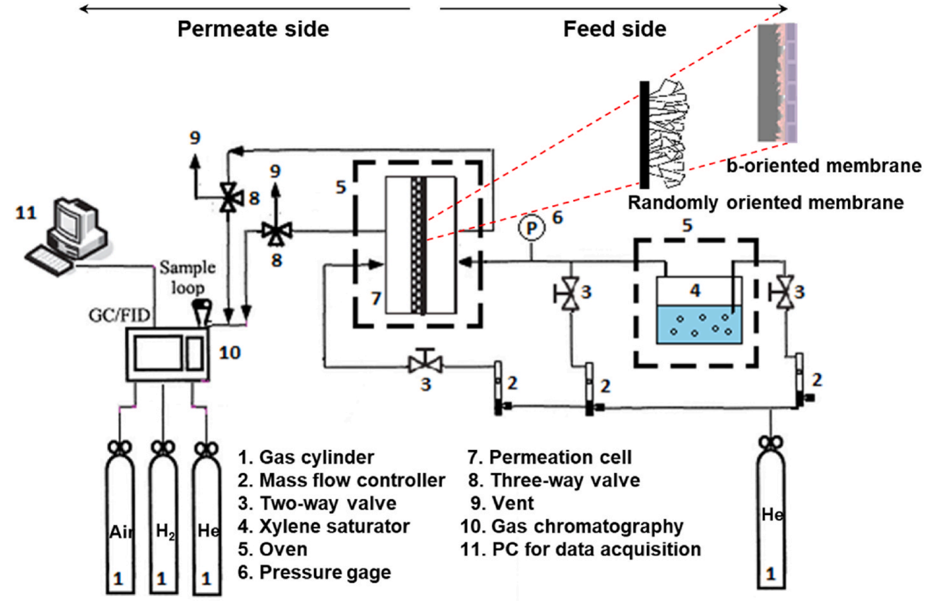

Fig. 2. Schematic diagram of xylene permeation/separation set up by vapor permeation experiments.

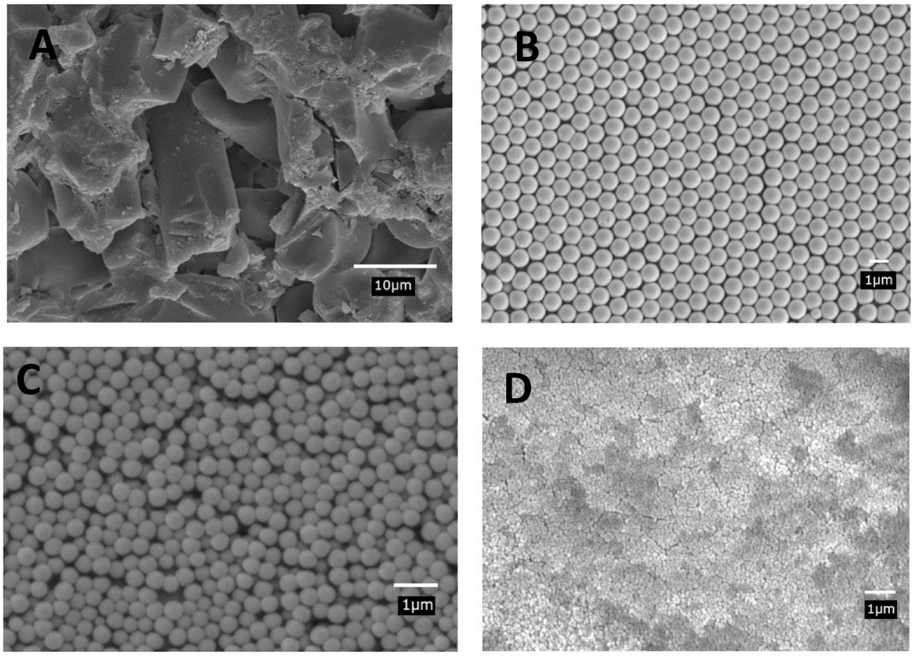

Fig. 3. SEM images of synthesized (A) silica fiber support, (B) 1 μm silica powder, (C) 350 nm silica powder, and (D) 50 nm silica powder.

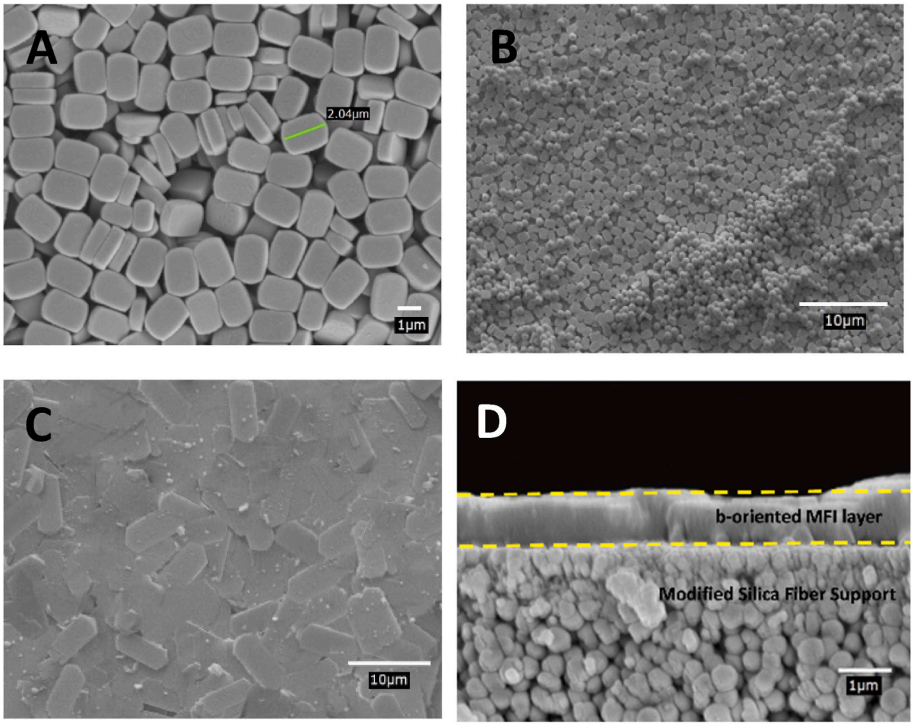

Fig. 4. (A) SEM image of synthesized coffin shaped crystals used for the seeding step of membrane preparation, (B) SEM image of the silica supports with seeded zeolite seeds; and (C) surface and cross sectional (D) SEM images of synthesized B-oriented membrane.

intercrystalline gaps (such as randomly oriented MFI zeolite membrane synthesized with an organic template), such temperature dependence of the xylene permeance and selectivity may not be as obvious due to the effect of intercrystalline pores on transport characteristics. Separation factor of p-xylene/o-xylene decreases by 28% and 31% for b-oriented and random templated membrane respectively. For templated randomly oriented MFI zeolite membrane, the o-xylene permeance through the intercrystalline gap is much higher than the b-oriented zeolite membrane. So, the good performance of as-prepared b-oriented membrane could be attributed to the highly intergrown MFI crystals in the zeolite layer and this limit the formation of non-selective permeation pathway through the membrane layer.

At a given temperature, vapor permeation separation of xylene isomers by the b-oriented MFI zeolite membrane shows decreasing permeance of xylene isomers with increasing xylene activity in the feed (Fig. 7). At 150 °C the highest p/o-xylene selectivity is 515, at a total xylene feed pressure of 1.06 kPa. The permeance of both p- and o-xylene decreases with increasing activity, but more so for p-xylene resulting in a

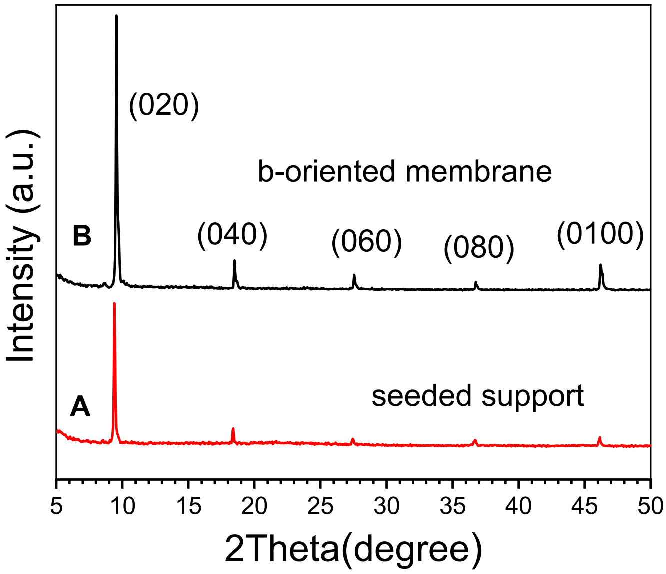

Fig. 5. XRD patterns of MFI zeolite seeded silica substrate (A) and b-oriented MFI zeolite membrane after secondary growth (B).

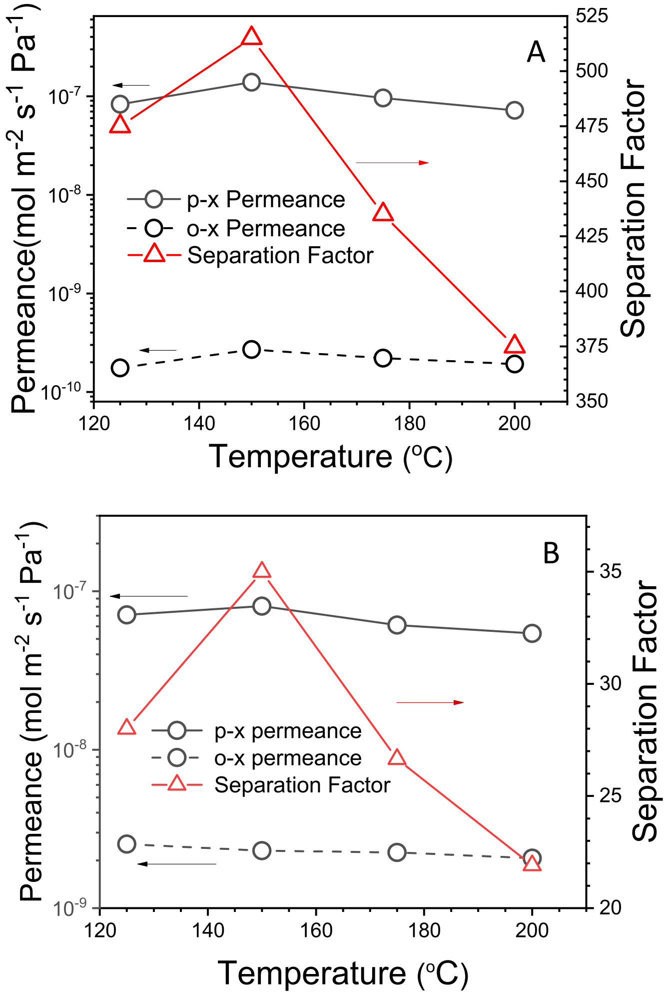

Fig. 6. Permeance and separation factor for (A) b-oriented (B) templated random oriented MFI zeolite membrane with binary p-xylene/o-xylene feed at different temperatures (at feed partial pressures of 0.56 kPa for p-xylene and 0.49 kPa for o-xylene).

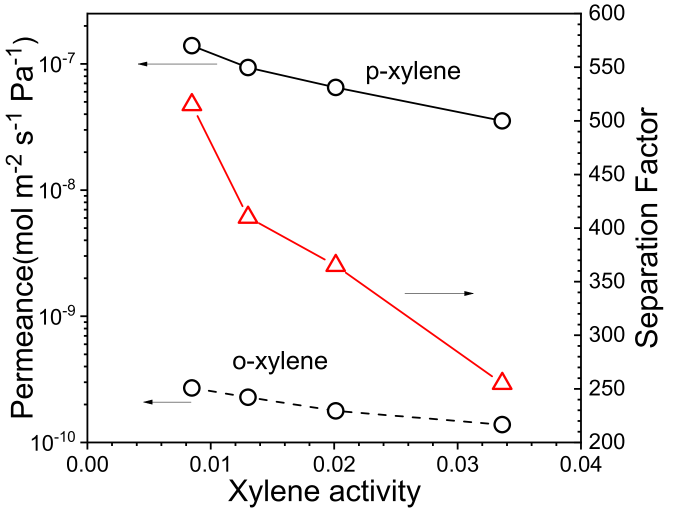

Fig. 7. Permeance and separation factor for b-oriented MFI zeolite membrane with binary p-xylene/o-xylene feed at different xylene vapor pressure (activity) at 150 °C.

decrease in p/o xylene selectivity with increasing activity. Similar xylene activity dependence of the permeance and selectivity for xylene isomers for randomly-oriented MFI zeolite membranes was reported by our group previously [15].

Single and multi-component pervaporation tests for p-xylene and o-xylene were performed at 25 °C for each membrane. Multiple runs of b-oriented MFI zeolite membranes are presented to ensure the high reproducibility of obtained pervaporation data. The pervaporation test results for the b-oriented membrane synthesized in this work are shown in Table 2. The driving force for pervaporation is the fugacity difference for the permeating species between the feed solution and permeate, i.e. ($X_iP_{i,sat} - Y_iP_{perm}$), where X_i and $P_{i,sat}$ are liquid phase molar fraction and statured vapor pressure of component i, and Y_i and P_{perm} are vapor phase molar fraction for species i and permeate pressure. In general, the permeate term in the driving force can be neglected so at a given temperature the pervaporation flux is proportional to the molar fraction of component i in the feed solution. This explains that the permeation flux for p- and o-xylenes with 50:50 binary feed is about a half of the flux for the pure xylene feed. The reduction of xylene permeation flux also is affected by the interaction between two components in the binary feed. In the case of MFI zeolite membranes, the main limitation of pervaporation separation of xylene isomers is ascribed to the high p-xylene loading in the MFI structure, especially at high xylene activity [22].

Compared to vapor separation data in Fig. 6, the results in Table 2 show that the b-oriented MFI zeolite membrane has much poorer separation performance in the pervaporation mode than in the vapor permeation mode. Pervaporation only gives p/o-xylene selectivity of about 2, significantly lower than the vapor permeation results. Similar results were obtained for vapor permeation and pervaporation

Table 2
Pervaporation performance of xylene isomer separation by b-oriented MFI Zeolite Membranes at 25 °C.

Mem #	Single-component flux (kg/m^2.h)		Multi-component flux(kg/m^2.h)		Separation capability	
	p-xylene flux	o-xylene flux	p-xylene flux	o-xylene flux	Ideal selectivity (p-x/o-x)	Mixture Separation factor α p-x/o-x
1	1.00	0.460	0.485	0.241	2.18	1.75
2	1.10	0.501	0.526	0.285	2.20	1.61
3	0.989	0.441	0.490	0.227	2.24	1.92

separation of xylene isomers by randomly oriented MFI zeolite membranes [15,18].

Fig. 8 shows temperature dependence of the pervaporation separation performance of the b-oriented MFI membrane for separation of equimolar p-xylene/o-xylene mixture. As the pervaporation temperature increases, the p-xylene flux increases but o-xylene flux decreases, leading to an increase in p-x/o-x separation factor. The increase of flux with increasing temperature is usually observed for microporous membranes in pervaporation [23,24]. This is because the driving force for pervaporation (vapor pressure in the feed) and diffusion rate increase with increasing temperature. This explains the temperature dependence of pervaporation flux for smaller p-xylene. The bulkier o-xylene may permeate mainly through intercrystalline gaps at a very slow rate. The intercrystalline gaps may decrease and hence o-xylene permeation flux with increasing temperature. Similar temperature dependence for o-xylene was also observed for vapor permeation. However, compared to the vapor permeation data, the xylene permeation flux and separation factor for b-oriented MFI zeolite membranes have a weaker temperature dependence in pervaporation mode.

Recently, we explained such separation factor decrease with increasing xylene vapor pressure (or activity) for MFI zeolite membranes by the effects of change in solubility and diffusivity of xylene, as well as presence of intercrystalline gaps and change of microstructure of MFI zeolite with increasing xylene loading in the zeolite due to increasing xylene activity [15]. For vapor permeation, the separation factor decreases with increasing xylene activity. Since pervaporation separation is equivalent to vapor permeation at highest activity (equal to 1), it is expected that the membrane operated in the pervaporation mode has lowest separation factor.

For vapor permeation at high xylene activity or pervaporation, MFI zeolite crystalline pores are filled with a high loading of p-xylene molecules (up to 8 m.u.c) [9]. At such high p-xylene loading, the MFI zeolite crystal could experience an overall expansion of 0.39% with a- and c-axis expansion of 0.09% and 0.52%, respectively, and b-axis contraction of 0.23% [25]. This may change the membrane structure of polycrystalline MFI zeolite (intercrystalline gaps or crystal orientation). Fig. 9 shows the structure change in the b-oriented MFI membrane during pervaporation test. The XRD patterns of b-oriented membrane before and after the pervaporation test are presented in Fig. 9A. XRD pattern of fresh b-oriented membrane shows five distinct diffraction peaks at 8.89°,17.8°, 26.82°, 36.06°, and 45.46°, attributed to the (020), (040), (060), (080), and (0100) crystal faces of MFI zeolite. The XRD pattern for the same membrane after pervaporation test shows two more peaks at 8.04° and between 23° and 24° which also can be seen in the random membrane XRD pattern. In addition, the intensity of the b-oriented peaks especially in (020) deflection for the membrane decreases significantly for pervaporation test. The microstructure of the b-oriented zeolite membranes appears more susceptible to crack formation during pervaporation experiments as shown in the picture (Fig. 9B) obtained by an Olympus MX50 optical microscope with the magnification of 250x. Such cracks were less likely to form for the randomly oriented MFI zeolite membranes after xylene permeation tests [4,15,18].

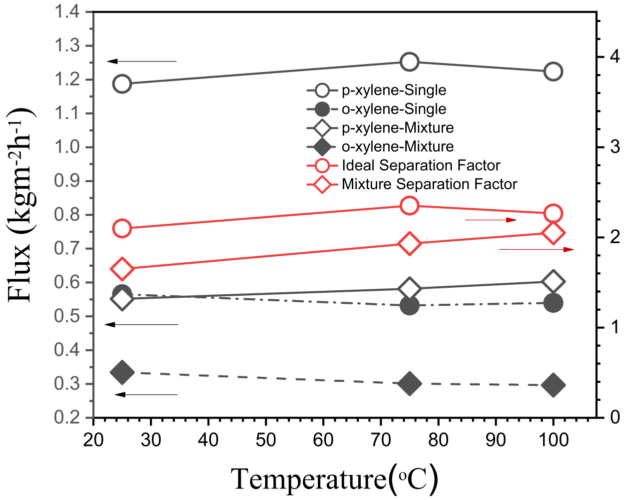

Fig. 8. Pervaporation flux and separation factor for b-oriented MFI zeolite membrane with single and binary p-xylene/o-xylene feed at different temperature.

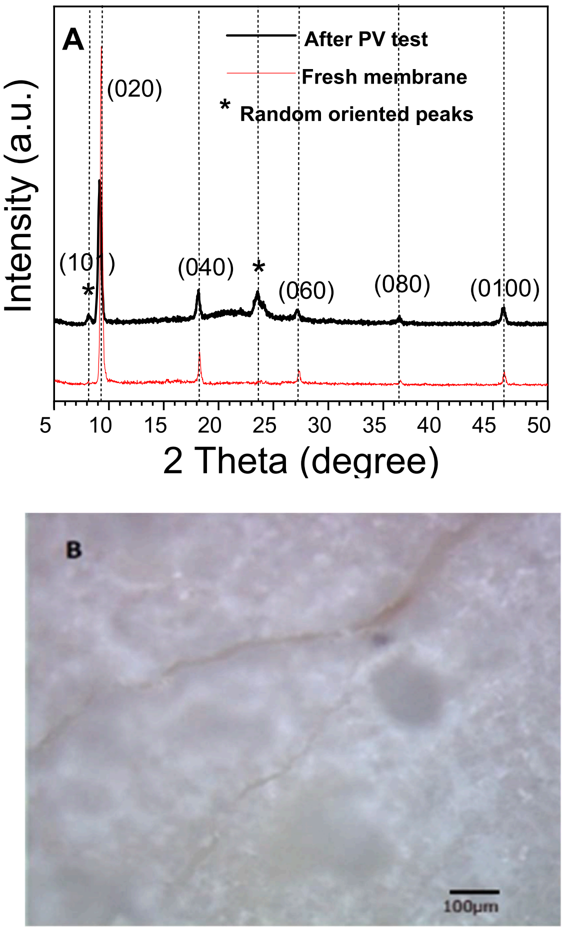

Fig. 9. Structure change of b-oriented membrane after pervaporation test (A) XRD patterns (B) Microscopic image of membrane surface after test.

Table 3 compares vapor permeation and pervaporation separation properties of p-xylene/o-xylene mixture by b-oriented MFI zeolite membrane prepared in this work and those of our previously reported

Table 3

Comparison of Xylene Vapor Permeation and Pervaporation Properties of b-oriented and randomly oriented MFI zeolite membranes both prepared with organic template.

Membrane	Observed Thickness (μm)	Vapor permeation (T = 150°C, P_{xylene}~0.5 kPa)		Pervaporation (T = 25°C)	
		p-xylene permeance ($mol/m^2.s.Pa$)	p-/o-xylene separation factor	p-xylene flux ($kg/m^2.h$)	p-/o-xylene separation factor
b-oriented	1.2	$1.4x10^{-7}$	515	0.50	1.8
Randomly-oriented [15]	9.7	$0.9x10^{-7}$	31	0.27	1.9

randomly oriented MFI zeolite membrane[15]. It should be noted that the observed thickness for randomly oriented MFI zeolite membrane may include portion of zeolite membrane with large intercrystalline gaps so the actual thickness of dense region could be smaller. Both membranes were synthesized with organic template so removal of the template could create or enlarge intercrystalline gaps [15,18,26,27]. The b-oriented zeolite membranes show better vapor permeation separation characteristics and larger pervaporation flux due to smaller membrane thickness, less intercrystalline gaps and more preferred crystal orientation than the randomly oriented zeolite membranes. However, for both membranes the xylene separation factor drops significantly in the pervaporation mode. In fact, they have essentially same p-/o-xylene separation factor despite that the b-oriented zeolite membrane has much better vapor separation characteristics than the randomly oriented one.

Fig. 10 compares the dependence of p-xylene vapor permeance and p/o-xylene separation factor of the b-oriented MFI zeolite membrane with the randomly oriented MFI zeolite membrane prepared in our lab [15]. The p-/o-xylene selectivity for MFI zeolite can be correlated to [15]:

$$\alpha_{p/o} = \left[\frac{F_p^{ZIF}}{F_o^{ZIF}}\right]\left[\frac{1}{1+\frac{F^{Int}}{F_o^{ZIF}}}\right] \qquad (1)$$

where F_p^{ZIF} and F_o^{ZIF} are permeance for p- and o-xylene through intracrystalline zeolite, which depends on the xylene activity, and F^{Int} is the Knudsen permeance through intercrystalline pores (same for both p- and o-xylenes) with a weak xylene activity dependence. At low xylene activity (about 0.01) and 150°C, the p-xylene permeance and p-/o-xylene separation factors for the b-oriented zeolite membrane are much larger than that for the randomly oriented zeolite membrane (see Table 3). These results suggest that the b-oriented zeolite membrane has much smaller/less intercrystalline gaps and hence smaller F^{Int} than the randomly oriented zeolite membrane. As a result, as the xylene activity increases both F_p^{ZIF} and F_o^{ZIF} decrease for both membranes, but with a smaller F^{Int} the impact of the 2nd term in Eq. (1) on the observed selectivity due to increased activity is smaller for the b-oriented MFI zeolite membrane than for the randomly-oriented MFI zeolite membrane. This explains the activity dependence of separation factor shown in Fig. 10.

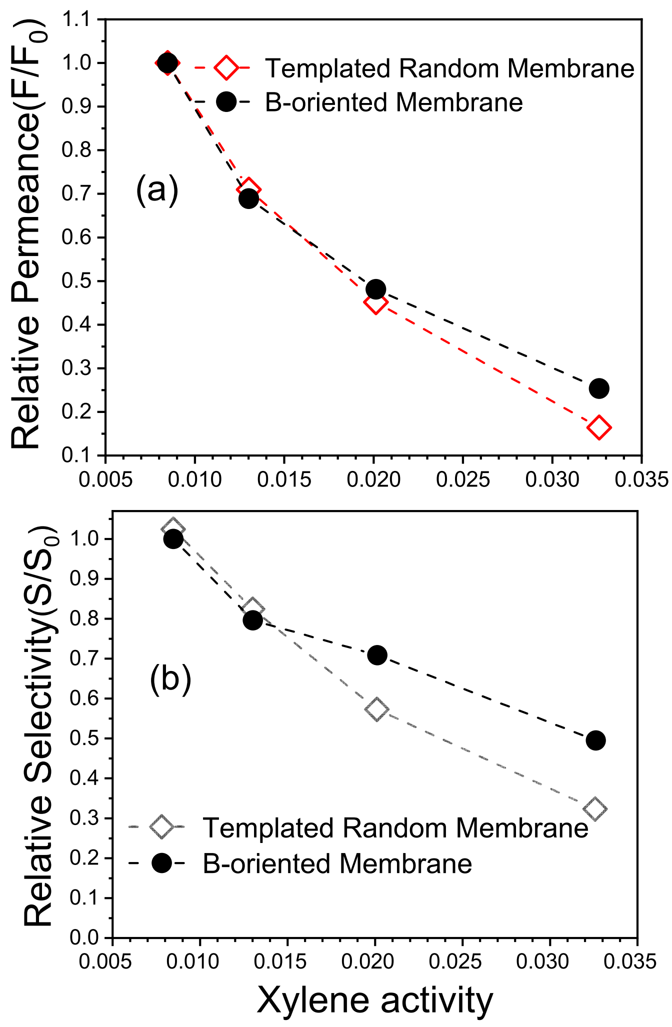

Fig. 10. Effect of xylene activity on (a) p-xylene permeance and (b) p/o-xylene selectivity for templated randomly oriented and templated b-oriented MFI zeolite membranes (50:50 p-xylene: o-xylene mixture feed, at 150 °C).

The unfavourable xylene activity dependence of the xylene separation performance of both b- and randomly oriented MFI zeolite membranes reported here show a challenge in using MFI zeolite membranes for industrial xylene separation applications. These results indicate that intercrystalline structure has a strong effect on xylene activity dependence of xylene separation characteristics of polycrystalline MFI zeolite membranes. The present work suggests more research efforts in synthesis of polycrystalline MFI zeolite membranes with framework and intercrystalline pore structures more resistant to the negative effect of p-xylene loading on xylene separation performance through e.g., isomorphous framework ion-substitution or template-free synthesis of MFI zeolite membrane.

4. Conclusions

Xylene vapor permeation/separation data confirm that b-oriented MFI zeolite membranes with a highly intergrown zeolite layer and low non zeolitic defect can be synthesized by the seeded-secondary gel-free method. Comparing the b-oriented and templated randomly oriented MFI zeolite membranes, the latter have larger intercrystalline xylene permeance than the former. Xylene vapor permeance and p-/o-xylene separation factor decrease with increasing xylene activity for both MFI zeolite membranes. The decrease in p-xylene intracrystalline permeance due to increase in activity has a more pronounced influence on separation factor. The negative activity dependence of p-/o-xylene vapor separation factor is more significant for the templated randomly oriented MFI zeolite membrane than the b-oriented MFI zeolite membrane due to difference in the microstructure. However, both membranes exhibit a similarly poor separation factor when operated in the pervaporation mode. These results can be explained qualitatively by the increasing p-xylene loading and change in the intercrystalline pore structure with increasing xylene activity. Xylene permeance and separation factor for the b-oriented MFI zeolite membrane have a stronger temperature dependence when operated in vapor permeation mode than in pervaporation mode.

CRediT authorship contribution statement

Fateme Banihashemi: Investigation, Formal analysis, Data curation, Methodology, Writing – original draft, preparation. **Jerry Y.S. Lin:** Methodology, Formal analysis, Resources, Supervision, Project administration, Funding acquisition, Writing – review & editing.

Declaration of competing interest

The authors declare that they have no known competing financial interests or personal relationships that could have appeared to influence the work reported in this paper.

Acknowledgments

The authors gratefully acknowledge the financial support from National Science Foundation of the United States (CBET-2031087).

References

[1] J. Čejka, Metal-organic frameworks. Applications from catalysis to gas storage, in: David Farrusseng (Ed.), Angew. Chem. Int. Ed. 51 (2012) 4782–4783, https://doi.org/10.1002/anie.201200812.

[2] M.I. Gonzalez, M.T. Kapelewski, E.D. Bloch, P.J. Milner, D.A. Reed, M.R. Hudson, J.A. Mason, G. Barin, C.M. Brown, J.R. Long, Separation of xylene isomers through multiple metal site interactions in metal–organic frameworks, J. Am. Chem. Soc. 140 (2018) 3412–3422, https://doi.org/10.1021/jacs.7b13825.

[3] Y.Y. Fong, A.Z. Abdullah, A.L. Ahmad, S. Bhatia, Development of functionalized zeolite membrane and its potential role as reactor combined separator for para-xylene production from xylene isomers, Chem. Eng. J. 139 (2008) 172–193, https://doi.org/10.1016/j.cej.2007.10.019.

[4] J. O'Brien-Abraham, Y.S. Lin, Effect of isomorphous metal substitution in zeolite framework on pervaporation xylene-separation performance of MFI-type zeolite membranes, Ind. Eng. Chem. Res. 49 (2010) 809–816, https://doi.org/10.1021/ie900926t.

[5] M.Y. Jeon, D. Kim, P. Kumar, P.S. Lee, N. Rangnekar, P. Bai, M. Shete, B. Elyassi, H. S. Lee, K. Narasimharao, S.N. Basahel, S. Al-Thabaiti, W. Xu, H.J. Cho, E.O. Fetisov, R. Thyagarajan, R.F. DeJaco, W. Fan, K.A. Mkhoyan, J.I. Siepmann, M. Tsapatsis, Ultra-selective high-flux membranes from directly synthesized zeolite nanosheets, Nature 543 (2017) 690–694, https://doi.org/10.1038/nature21421.

[6] J. Caro, M. Noack, J. Richter-Mendau, F. Marlow, D. Petersohn, M. Griepentrog, J. Kornatowski, Selective sorption uptake kinetics of n-hexane on ZSM 5 - a new method for measuring anisotropic diffusivities, Am. J. Phys. Chem. 97 (1993) 13685–13690, https://doi.org/10.1021/j100153a043.

[7] J. Kaerger, Random walk through two-channel networks: a simple means to correlate the coefficients of anisotropic diffusion in ZSM-5 type zeolites, J. Phys. Chem. 95 (1991) 5558–5560, https://doi.org/10.1021/j100167a036.

[8] M.A. Snyder, M. Tsapatsis, Hierarchical nanomanufacturing: from shaped zeolite nanoparticles to high-performance separation membranes, Angew. Chem. Int. Ed. 46 (2007) 7560–7573, https://doi.org/10.1002/anie.200604910.

[9] G. Xomeritakis, S. Nair, M. Tsapatsis, Transport properties of alumina-supported MFI membranes made by secondary (seeded) growth, Microporous Mesoporous Mater 38 (2000) 61–73, https://doi.org/10.1016/S1387-1811(99)00300-5.

[10] T.C.T. Pham, H.S. Kim, K.B. Yoon, Growth of uniformly oriented silica MFI and BEA zeolite films on substrates, Science 334 (2011) 1533–1538, https://doi.org/10.1126/science.1212472.

[11] T.C.T. Pham, T.H. Nguyen, K.B. Yoon, Gel-free secondary growth of uniformly oriented silica MFI zeolite films and application for xylene separation, Angew. Chem. Int. Ed. 52 (2013) 8693–8698, https://doi.org/10.1002/anie.201301766.

[12] Z. Lai, M. Tsapatsis, J.J.A.F.M. Nicolich, Siliceous ZSm 5 membranes by secondary growth of b oriented seed layers, Adv. Funct. Mater. 14 (2004) 716–729, https://doi.org/10.1002/adfm.200400040.

[13] K.V. Agrawal, B. Topuz, T.C.T. Pham, T.H. Nguyen, N. Sauer, N. Rangnekar, H. Zhang, K. Narasimharao, S.N. Basahel, L.F. Francis, C.W. Macosko, S. Al-Thabaiti, M. Tsapatsis, K.B. Yoon, Oriented MFI membranes by gel-less secondary growth of sub-100 nm MFI-nanosheet seed layers, Adv. Mater. 27 (2015) 3243–3249, https://doi.org/10.1002/adma.201405893.

[14] D. Kim, M.Y. Jeon, B.L. Stottrup, M. Tsapatsis, para-Xylene ultra-selective zeolite MFI membranes fabricated from nanosheet monolayers at the air–water interface, Angew. Chem. Int. Ed. 57 (2018) 480–485, https://doi.org/10.1002/anie.201708835.

[15] F. Banihashemi, L. Meng, A.A. Babaluo, Y.S. Lin, Xylene vapor permeation in MFI zeolite membranes made by templated and template-free secondary growth of randomly oriented seeds: effects of xylene activity and microstructure, Ind. Eng. Chem. Res. 57 (2018) 16059–16068, https://doi.org/10.1021/acs.iecr.8b01373.

[16] C.J. Gump, V.A. Tuan, R.D. Noble, J.L. Falconer, Aromatic permeation through crystalline molecular sieve membranes, Ind. Eng. Chem. Res. 40 (2001) 565–577, https://doi.org/10.1021/ie000553i.

[17] X. Gu, J. Dong, T.M. Nenoff, D.E. Ozokwelu, Separation of p-Xylene from multicomponent vapor mixtures using tubular MFI zeolite membranes, J. Membr. Sci. 280 (2007) 624–633, https://doi.org/10.1016/S0167-2991(07)80944-X.

[18] J. O'Brien-Abraham, M. Kanezashi, Y.S. Lin, Effects of adsorption-induced microstructural changes on separation of xylene isomers through MFI-type zeolite membranes, J. Membr. Sci. 320 (2008) 505–513, https://doi.org/10.1016/j.memsci.2008.04.023.

[19] W. Stöber, A. Fink, E. Bohn, Controlled growth of monodisperse silica spheres in the micron size range, J. Colloid Interface Sci. 26 (1968) 62–69, https://doi.org/10.1016/0021-9797(68)90272-5.

[20] B. Elyassi, M.Y. Jeon, M. Tsapatsis, K. Narasimharao, S.N. Basahel, S. Al-Thabaiti, Ethanol/water mixture pervaporation performance of b-oriented silicalite-1 membranes made by gel-free secondary growth, AIChE J 62 (2016) 556–563, https://doi.org/10.1002/aic.15124.

[21] F. Banihashemi, A.F.M. Ibrahim, A.A. Babaluo, J.Y.S. Lin, Template-free synthesis of highly b-oriented MFI-type zeolite thin films by seeded secondary growth, Angew. Chem. Int. Ed. 58 (2019) 2519–2523, https://doi.org/10.1002/anie.201814248.

[22] M.O. Daramola, Z. Deng, M. Pera-Titus, A. Giroir-Fendler, S. Miachon, A.J. Burger, L. Lorenzen, Y. Guo, Nanocomposite MFI–alumina membranes prepared via pore-pugging synthesis: application as packed-bed membrane reactors for m-xylene isomerization over a Pt-HZSM-5 catalyst, Catal. Today 156 (2010) 261–267, https://doi.org/10.1016/j.cattod.2010.03.077.

[23] X. Wu, W. Wei, J. Jiang, J. Caro, A. Huang, High-flux high-selectivity metal–organic framework MIL-160 membrane for xylene isomer separation by, Pervaporation 57 (2018) 15354–15358, https://doi.org/10.1002/anie.201807935.

[24] H. Guo, Z. Wan, Y. Li, X. He, A. Huang, Synthesis of graphene oxide membrane for separation of p-xylene and o-xylene by, Pervaporation 94 (2022) 78–85, https://doi.org/10.1002/cite.202100084.

[25] B.F. Mentzen, P. Gelin, The silicalite/p-xylene system : Part I — flexibility of the MFI framework and sorption mechanism observed during p-xylene pore-filling by X-ray powder diffraction at room temperature, Mater. Res. Bull. 30 (1995) 373–380, https://doi.org/10.1016/0025-5408(95)00003-8.

[26] M. Kanezashi, J. O'Brien, Y.S. Lin, Template-free synthesis of MFI-type zeolite membranes: permeation characteristics and thermal stability improvement of membrane structure, J. Membr. Sci. 286 (2006) 213–222, https://doi.org/10.1016/j.memsci.2006.09.038.

[27] J.L. O'Brien-Abraham, M. Kanezashi, Y.S. Lin, Effect of microstructure of MFI-type zeolite membranes on separation of xylene isomers, in: R. Xu, Z. Gao, J. Chen, W. Yan (Eds.), Studies in Surface Science and Catalysis, Elsevier, 2007, pp. 967–974, https://doi.org/10.1016/S0167-2991(07)80947-5.